Numerical solution of a phase field model for polycrystallization processes in binary mixtures

Ronald H. W. Hoppe[1,2] · James J. Winkle[2]

Abstract
We consider the numerical solution of a phase field model for polycrystallization in the solidification of binary mixtures in a domain $\Omega \subset \mathbb{R}^2$. The model is based on a free energy in terms of three order parameters: the local orientation Θ of the crystals, the local crystallinity ϕ, and the concentration c of one of the components of the binary mixture. The equations of motion are given by an initial-boundary value problem for a coupled system of partial differential equations consisting of a regularized second order total variation flow in Θ, an L^2 gradient flow in ϕ, and a $W^{1,2}(\Omega)^*$ gradient flow in c. Based on an implicit discretization in time by the backward Euler scheme, we suggest a splitting method such that the three semidiscretized equations can be solved separately and prove existence of a solution. As far as the discretization in space is concerned, the fourth order Cahn–Hilliard type equation in c is taken care of by a C^0 Interior Penalty Discontinuous Galerkin approximation which has the advantage that the same finite element space can be used as well for the spatial discretization of the equations in Θ and ϕ. The fully discretized equations represent parameter dependent nonlinear algebraic systems with the discrete time as a parameter. They are solved by a predictor corrector continuation strategy featuring an adaptive choice of the time-step. Numerical results illustrate the performance of the suggested numerical method.

1 Introduction

Polycrystallization involves several mechanisms that occur in the solidification of materials on a microscale such as the nucleation of crystals, the formation of spherulites, and the growth of mosaic eutectic structures. The mathematical modeling of multistage crystallization processes can be done by a phase field approach based on a free energy in terms of various order parameters (cf., e.g., the monograph [43] as well as the survey papers [25,28] and the references therein). An important order parameter for modeling the complex crystalline morphology is the orientation field which monitors the local crystallographic orientation. The first orientation field phase field model has been developed by Kobayashi, Warren, and Carter [31,47] describing the growth of anisotropic single-crystal particles of different orientations in two dimensions. The free energy involves two order parameters describing the local orientation angle and the local degree of crystallinity. The equations of motion are given by an L^2 gradient flow and a total variation flow. An extension of that model for the polyystallization of binary alloys has been provided by Granasy et al. where the free energy is given in terms of an orientation field, the local degree of crystallinity, and a concentration field which describes the volume fraction of one of the components of the binary mixture (cf. [22,23]; see also [24,26,27]). The equations of motion are given by an initial-boundary value problem for a coupled system of partial differential equations consisting of two nonlinear second order parabolic equations (in the orientation and the local degree of crystallinity) and one nonlinear fourth order parabolic equation of Cahn–Hilliard type (in the concentration). We note that Cahn–Hilliard systems for phase separation taking into account mechanical effects such as the Cahn–Larché system [32–34] have been intensively investigated in the literature (see [6,10,14,15,19,20,29,35–

J. J. Winkle: The authors acknowledge support by the NSF Grant DMS-1520886.

✉ Ronald H. W. Hoppe
ronald.h.w.hoppe@math.uni-augsburg.de

[1] Institute of Mathematics, University of Augsburg, 86159 Augsburg, Germany

[2] Department of Mathematics, University of Houston, Houston, TX 77204-3008, USA

39]). In particular, [19] analyzes the Cahn–Larché system as a $W^{1,2}(\Omega)^*$ gradient flow. Likewise, the total variation flow and its regularization have been widely studied as well (cf., e.g., [1–3,8,9,13,18,45]).

In this paper, we will study the numerical solution of a slightly modified version of this model which consists in replacing the total variation flow of the orientational field by some regularized version. The paper is organized as follows: In Sect. 2, we specify the free energy associated with the three field phase field model as well as the equations of motion and introduce the concept of a weak solution. Following [19], we formulate the equation of motion for the concentration field as a $W^{1,2}(\Omega)^*$ gradient field. In Sect. 3, we perform an implicit time discretization and splitting of the phase field model. The splitting allows to consider the orientation field, the phase field representing the local degree of crystallinity, and the concentration field separately at each time step. In fact, it is shown that the time-discrete equations represent the necessary optimality conditions for the minimization of energy functionals assigned to each time step. Section 4 is devoted to the discretization in space. The fourth order Cahn–Hilliard type equation is discretized by a (nonconforming) C^0 Interior Penalty Discontinuous Galerkin (C^0IPDG) approximation (cf., e.g., [11,12,17,48]. The advantage is that the same finite element space can be used for a spatial discretization of the orientation field and the phase field representing the local degree of crystallinity. The fully discretized equations can be seen as parameter dependent nonlinear algebraic equations with the discrete time as the parameter. For the numerical solution, in Sect. 5 we suggest a predictor corrector continuation strategy featuring an adaptive choice of the time step size (cf. [16,30]). Finally, in Sect. 6 we present some numerical results illustrating the performance of the suggested splitting method.

Throughout this paper, we use standard notation and results from Lebesgue and Sobolev space theory (cf., e.g., [46]). Moreover, for a positive weight function ω we denote by $BV(\Omega;\omega)$ the Banach space of functions of bounded weighted total variation (cf. [4,21])

$$\mathrm{var}_\omega u(\Omega) := \sup\left\{ -\int_\Omega u \nabla\cdot \mathbf{q}\, dx, \quad \mathbf{q}\in C_0^1(\Omega;\mathbb{R}^2),\ |\mathbf{q}|\le \omega \text{ in } \Omega \right\},$$

equipped with the norm

$$\|u\|_{BV(\Omega;\omega)} := \int_\Omega \omega|u|\, dx + \mathrm{var}_\omega u(\Omega).$$

2 The phase field model

For the mathematical modeling of the polycrystallization of binary mixtures we use a phase field approach where the free energy functional is given in terms of

- an orientation field Θ which locally describes the crystallographic orientation.
- a structural order parameter ϕ which measures the local crystallinity (volume fraction of the crystalline phase),
- a concentration field c (volume fraction of one of the components of the binary mixture).

Setting $z = (\phi, c, \Theta)$, the free energy reads as follows:

$$\begin{aligned} F(z) = \int_\Omega \Big(& \frac{\varepsilon_\phi^2 T}{2}\, s(\nabla\phi,\Theta)^2\, |\nabla\phi|^2 + \frac{\varepsilon_c^2 T}{2}\, |\nabla c|^2 \\ & + w(c) T g(\phi) + \omega(\phi)(f_S(c,T) \\ & + HT\ (\kappa_\Theta + |\nabla\Theta|^2)^{1/2} \\ & + (1-\omega(\phi))\, f_L(c,T))\ dx. \end{aligned} \tag{1}$$

Here, $\Omega\subset\mathbb{R}^2$ is assumed to be a bounded convex domain with boundary $\Gamma = \partial\Omega$ of class C^2. Moreover, T (in ^{0}K) refers to the temperature of the binary mixture.
$f_L(\cdot,T)$ and $f_S(\cdot,T)$ stand for the Helmholtz free energy densities of the pure liquid and the pure solid phase

$$\begin{aligned} f_L(\eta,T) &:= \frac{W_L}{4}\eta^2\left(\eta^2 - \frac{4}{3}\left(\frac{3}{2}+\beta_L(T)\right)\eta \right. \\ &\quad \left. +2\left(\frac{1}{2}+\beta_L(T)\right)\right), \quad \eta\in\mathbb{R}, \\ \beta_L(T) &:= \beta_L \frac{T - T_M^{(L)}}{T_M^{(L)}}, \\ f_S(\eta,T) &:= \frac{W_S}{4}\eta^2\Big(\eta^2 - \frac{4}{3}\Big(\frac{3}{2}+\beta_S(T)\Big)\eta \\ &\quad + 2\Big(\frac{1}{2}+\beta_S(T)\Big)\Big), \quad \eta\in\mathbb{R}, \\ \beta_S(T) &:= \beta_S \frac{T - T_M^{(S)}}{T_M^{(S)}}, \end{aligned} \tag{2}$$

where $T_M^{(L)}$ and $T_M^{(S)}$ are the melting temperatures of the components of the binary mixture and $W_L > 0$, $W_S > 0$ as well as $\beta_L > 0$, $\beta_S > 0$ are scaling parameters. We assume that

$$T_M^{(L)} < T < T_M^{(S)}$$

On the other hand, we may split $f_S(\cdot,T)$ according to

$$f_S(\eta,T) = f_{S,1}(\eta,T) + f_{S,2}(\eta,T), \tag{3}$$

where $f_{S,i}(\eta, T)$, $1 \le i \le 2$, $\eta \in \mathbb{R}$, are given by

$$f_{S,1}(\eta, T) := \frac{W_S}{4}\eta^2\Big(\eta^2 - \frac{4}{3}\Big(\frac{3}{2} + \beta(T)\Big)\eta + 2\Big(\frac{1}{2} + \beta(T)\Big) + a\Big),$$
$$f_{S,2}(\eta, T) := -\frac{W_S}{4}a\eta^2,$$

and $a \in \mathbb{R}$ is chosen by means of

$$a > \frac{2}{9}\beta_S(T)\left(\beta_S(T) - \frac{3}{2}\right).$$

The function $s = s(\boldsymbol{\eta}, \gamma)$, $\boldsymbol{\eta} = (\eta_1, \eta_2)^T \in \mathbb{R}^2, \gamma \in \mathbb{R}$, refers to the anisotropy function

$$s(\boldsymbol{\eta}, \gamma) = 1 + s_0 \cos(m_s\vartheta - 2\pi\gamma),$$
$$\vartheta = \begin{cases} \pi/2 & \text{if } \eta_1 = 0, \\ \arctan(\chi_{\varepsilon_a}(\eta_2/\eta_1)) & \text{otherwise} \end{cases} \tag{4}$$

Here, $0 \le s_0 \ll 1$ is the amplitude of the anisotropy of the interface free energy, m_s is the symmetry index (e.g., $m_s = 4$ for fourfold symmetry), and $\chi_{\varepsilon_a} \in C^2(\mathbb{R})$, $0 < \varepsilon_a \le 1$, is a smooth approximation of $\chi(x) = |x|$, $x \in \mathbb{R}$, with $\chi_{\varepsilon_a}(x) = \chi(x)$, $|x| \ge \varepsilon_a$, $\chi'_{\varepsilon_a}(\pm\varepsilon_a) = \pm 1$, $\chi''_{\varepsilon_a}(\pm\varepsilon_a) = 0$, and $\chi_{\varepsilon_a}(0) = 0$, e.g., we may choose

$$\chi_{\varepsilon_a}(x) = \begin{cases} |x| & |x| \ge \varepsilon_a \\ \frac{15}{8}\varepsilon_a^{-1}x^2 - \frac{5}{4}\varepsilon_a^{-3}x^4 + \frac{3}{8}\varepsilon_a^{-5}x^6 & |x| \le \varepsilon_a \end{cases}.$$

We note that ϑ is related to the inclination of the normal vector of the interface in the laboratory frame. The function w is given by

$$w(\eta) = \begin{cases} w_L - \varepsilon_w & \eta \le -\varepsilon_w \\ \alpha_L + \beta_L\eta + \gamma_L\eta^2 + \delta_L\eta^3 & -\varepsilon_w \le \eta \le 0 \\ (1-\eta)w_L + \eta w_S & 0 \le \eta \le 1 \\ \alpha_R + \beta_R\eta + \gamma_R\eta^2 + \delta_R\eta^3 & 1 \le \eta \le 1 + \varepsilon_w \\ w_S + \varepsilon_w & 1 + \varepsilon_w \le \eta \end{cases},$$

where $w_S > w_L > 0$ are the free energy scales of the two components, the parameter ε_w satisfies $0 < \varepsilon_w \le w_L$, and

$$\alpha_L = w_L, \quad \beta_L = w_S - w_L,$$
$$\gamma_L = \varepsilon_w^{-2}(2\varepsilon_w(w_S - w_L) - 3\varepsilon_w),$$
$$\delta_L = \varepsilon_w^{-3}(\varepsilon_w(w_S - w_L) - 2\varepsilon_w),$$
$$\alpha_R = w_L - \varepsilon_w^{-2}(2\varepsilon_w(w_S - w_L) + (w_S - w_L) + 1),$$
$$\beta_R = \varepsilon_w^{-2}(\varepsilon_w^2 + 4\varepsilon_w + 3)(w_S - w_L),$$
$$\gamma_R = -\varepsilon_w^{-2}(2\varepsilon_w(w_S - w_L) + 3(w_S - w_L) - 3),$$
$$\delta_R = \varepsilon_w^{-2}((w_S - w_L) - 2).$$

The function g is the quartic double-well function

$$g(\eta) = \frac{1}{4}\,\eta^2\,(1-\eta)^2.$$

The function ω is given by

$$\omega(\eta) = \begin{cases} \varepsilon_r & \eta \le 0 \\ \varepsilon_r + 2(2 - 3\varepsilon_r)\eta^2 - 4(1-\varepsilon_r)\eta^3 + \eta^4 & 0 \le \eta \le 1 \\ 1 - \varepsilon_r & \eta \ge 1 \end{cases},$$

where $0 < \varepsilon_r \ll 1$, interpolating between $(0, \varepsilon_r)$ and $(1, 1-\varepsilon_r)$. Moreover, the constant $H > 0$ stands for the free energy of the low-angle grain boundaries and $0 < \kappa_\Theta \ll 1$ is a regularization parameter. We will comment on the choice of κ_Θ in Remark 4.1 below. Finally, ε_ϕ^2 and ε_c^2 are positive constants depending on the interface free energy, the interface thickness, and the melting points of the constituents of the mixture.

Remark 2.1 The integral $\int_\Omega(\kappa_\Theta + |\nabla\Theta|^2)^{1/2}\,dx$ in (1) can be interpreted as the regularized weighted total variation

$$\operatorname{var}_{\omega(\phi)}^{(\kappa_\Theta)}\Theta(\Omega) \tag{5}$$
$$:= \sup\left\{\int_\Omega(-\Theta\nabla\cdot\mathbf{q} + \kappa_\Theta^{1/2}(\omega(\phi) - |\mathbf{q}|^2)^{1/2}\,dx,\right.$$
$$\left.\mathbf{q} \in C_0^1(\Omega;\mathbb{R}^2),\ |\mathbf{q}| \le \omega(\phi) \text{ in } \Omega\right\}. \tag{6}$$

The following properties of the functions f_L, $f_{S,1}$, s, w, g, and ω will be frequently used in the subsequent sections

$$f_L(\eta, T) \ge 0, \quad f_{S,1}(\eta, T) \ge 0, \quad \eta \in \mathbb{R}, \tag{7a}$$
$$1 - s_0 \le s(\boldsymbol{\eta}, \gamma) \le 1 + s_0, \quad \boldsymbol{\eta} \in \mathbb{R}^2, \gamma \in \mathbb{R}, \tag{7b}$$
$$0 \le w_L - \varepsilon_w \le w(\eta) \le w_S + \varepsilon_w, \quad \eta \in \mathbb{R}, \tag{7c}$$
$$g(\eta) \ge 0, \quad \eta \in \mathbb{R}, \tag{7d}$$
$$\varepsilon_r \le \omega(\eta) \le 1 - \varepsilon_r, \quad \eta \in \mathbb{R}. \tag{7e}$$

Denoting by $M_\phi > 0$, $M_c > 0$, and $M_\Theta > 0$ the mobilities associated with the phase field variables ϕ, c, and Θ, the dynamics of the crystallization process are given by the evolution equations

$$\frac{\partial\phi}{\partial t} = -M_\phi\,\frac{\delta F}{\delta\phi}, \tag{8a}$$
$$\frac{\partial c}{\partial t} = \nabla\cdot\left(M_c\nabla\frac{\delta F}{\delta c}\right), \tag{8b}$$

$$\frac{\partial \Theta}{\partial t} = -M_\Theta \frac{\delta F}{\delta \Theta}, \tag{8c}$$

where $\frac{\delta F}{\delta \phi}$, $\frac{\delta F}{\delta c}$, and $\frac{\delta F}{\delta \Theta}$ are the partial Gâteaux derivatives of the free energy functional F with respect to the three phase field variables.

Computing the partial Gâteaux derivatives, the phase field model represents an initial-boundary value problem for a system of evolutionary partial differential equations consisting of two nonlinear second order parabolic equations in Θ and Φ coupled to a Cahn–Hilliard type equation in c. We refer to

$$\begin{aligned}
&\mu(\phi, c) = h(\phi, c) - \varepsilon_c^2 T \Delta c,\\
&h(\phi, c) := w'(c) T g(\phi) + \omega(\phi) f_S'(c, T)\\
&\qquad\qquad + (1 - \omega(\phi)) f_L'(c, T)
\end{aligned}$$

as the generalized chemical potential. We set $a(\boldsymbol{\eta}, \gamma) = (a_{ij}(\boldsymbol{\eta}, \gamma))_{i,j=1}^2$ with

$$\begin{aligned}
&a_{11}(\boldsymbol{\eta}) = a_{22}(\boldsymbol{\eta}, \gamma) = s(\boldsymbol{\eta}, \gamma)^2,\\
&a_{12}(\boldsymbol{\eta}, \gamma) = -a_{21}(\boldsymbol{\eta}, \gamma) = -s(\boldsymbol{\eta}, \gamma) \frac{\partial s(\boldsymbol{\eta}, \gamma)}{\partial \vartheta}.
\end{aligned}$$

We further define

$$\begin{aligned}
r(\phi, c, \Theta) &:= w(c) T g'(\phi) + \omega'(\phi) \Big(f_S(c, T)\\
&\qquad - f_L(c, T) + HT(\kappa_\Theta + |\nabla \Theta|^2)^{1/2} \Big),\\
z(\phi, \Theta) &:= s(\nabla \phi, \Theta) \frac{\partial s(\nabla \phi, \Theta)}{\partial \Theta},
\end{aligned}$$

and specify appropriate boundary conditions and initial conditions for all phase field variables. Setting $Q := \Omega \times (0, t_F)$, $\Sigma := \Gamma \times (0, t_F)$, where $t_F > 0$ is the final time, and specifying appropriate boundary conditions and initial conditions for all phase field variables, the initial-boundary problem reads

$$\begin{aligned}
\frac{\partial \Theta}{\partial t} &= M_\Theta H T \nabla \cdot (\omega(\phi)(\kappa_\Theta + |\nabla \Theta|^2)^{-1/2} \nabla \Theta) \qquad (9a)\\
&\quad + M_\Theta\, z(\phi, \Theta) |\nabla \phi|^2, \quad \text{in } Q,\\
\frac{\partial \phi}{\partial t} &= M_\phi \Big(\varepsilon_\phi^2 T \nabla \cdot (a(\nabla \phi, \Theta) \nabla \phi) - r(\phi, c, \Theta) \Big), \quad \text{in } Q \qquad (9b)\\
\frac{\partial c}{\partial t} &= \nabla \cdot (M_c \nabla \mu(\phi, c)) \text{ in } Q, \qquad (9c)\\
\mathbf{n}_\Gamma \cdot \omega(\phi)(\kappa_\Theta + |\nabla \Theta|^2)^{-1/2} \nabla \Theta &= 0 \quad \text{on } \Sigma, \qquad (9d)\\
\mathbf{n}_\Gamma \cdot a(\nabla \phi, \Theta) \nabla \phi &= 0 \quad \text{on } \Sigma, \qquad (9e)\\
\mathbf{n}_\Gamma \cdot \nabla c = 0,\ \mathbf{n}_\Gamma \cdot \nabla \mu(\phi, c) &= 0 \quad \text{on } \Sigma, \qquad (9f)\\
\Theta(\cdot, 0) = \Theta^0,\ \Phi(\cdot, 0) = \Phi^0,\ c(\cdot, 0) &= c^0 \text{ in } \Omega. \qquad (9g)
\end{aligned}$$

Remark 2.2 The system in the orientation angle Θ and the local degree of crystallinity ϕ, but without the concentration field c, is known as the Kobayashi–Warren–Carter model[31, 47]. The existence of a solution has been established in [40] by means of an implicit discretization in time of a relaxed system and a non-trivial passage to the limit (cf. also [41] for the existence of an energy-dissipative solution). However, to our best knowledge, the existence of a solution of the full system (9a)–(9g) has not yet been shown.

Remark 2.3 We note that the Gauss' theorem and the second boundary condition in (9e) imply the existence of a constant $c_{av} \in \mathbb{R}$ such that $|\Omega|^{-1} \int_\Omega c(x, t)\, dt = c_{av}$ for almost all $t \in (0, T]$.

A weak solution of (9a)–(9g) is a quadruple (Θ, ϕ, c, w) such that

$$\begin{aligned}
&\Theta \in W^{1,1}(\Omega), \quad \phi, c, w \in W^{1,2}(\Omega),\\
&\frac{\partial \Theta}{\partial t}, \frac{\partial \phi}{\partial t}, \frac{\partial c}{\partial t} \in L^2(\Omega)
\end{aligned}$$

and for all

$$v_1 \in W^{1,1}(\Omega), \quad v_i \in W^{1,2}(\Omega), 2 \le i \le 4,$$

it holds

$$\begin{aligned}
&\left(\frac{\partial \Theta}{\partial t}, v_1 \right)_{0,\Omega} + M_\Theta H T (\omega(\phi)(\kappa_\Theta\\
&\quad + |\nabla \Theta|^2)^{-1/2} \nabla \Theta, \nabla v_1)_{0,\Omega}\\
&\quad - M_\Theta (z(\phi, \Theta) |\nabla \phi|^2, v_1)_{0,\Omega} = 0,\\
&\left(\frac{\partial \phi}{\partial t}, v_2 \right)_{0,\Omega} + M_\phi \Big(\varepsilon_\phi^2 T (a(\nabla \phi, \Theta) \nabla \phi, \nabla v_2)_{0,\Omega}\\
&\quad + (r(\phi, c, \Theta), v_2)_{0,\Omega} \Big) = 0,\\
&\left(\frac{\partial c}{\partial t}, v_3 \right)_{0,\Omega} + M_c (\nabla w, \nabla v_3)_{0,\Omega} = 0,\\
&(w, v_4)_{0,\Omega} = \varepsilon_c^2 T (\nabla c, \nabla v_4)_{0,\Omega} + (h(\phi, c), v_4)_{0,\Omega}.
\end{aligned}$$

The Cahn–Hilliard type equation (9c) can be written as a $W^{1,2}(\Omega)^*$-gradient flow with respect to a specific inner product. We define $\Delta^{-1} f$, $f \in W^{1,2}(\Omega)^*$, as the solution $u \in W^{1,2}(\Omega)$ of

$$-(\nabla u, \nabla v)_{0,\Omega} = \langle f, v \rangle_{W^{1,2}(\Omega)^*, W^{1,2}(\Omega)}, \quad v \in W^{1,2}(\Omega).$$

The unique solvability follows from the Lax–Milgram Lemma in virtue of the Poincaré-Wirtinger inequality for convex domains [7,42]

$$\| v - |\Omega|^{-1} \int_\Omega v\, dx \|_{0,\Omega} \le \frac{1}{\pi^2} \| \nabla v \|_{0,\Omega}, \quad v \in W^{1,2}(\Omega).$$

We define an inner product on $W^{1,2}(\Omega)^*$ according to

$$(f,g)_{\Delta^{-1}} := (\nabla\Delta^{-1}f, \nabla\Delta^{-1}g)_{0,\Omega}. \tag{10}$$

Using Young's inequality with $\varepsilon > 0$, for $u \in W^{1,2}(\Omega)$ we find

$$\begin{aligned}\|u\|^2_{0,\Omega} &= (\nabla u, \nabla\Delta^{-1}u)_{0,\Omega}\\ &\le \|\nabla u\|_{0,\Omega}\|\nabla\Delta^{-1}u\|_{0,\Omega} \le \varepsilon\|\nabla u\|^2_{0,\Omega} + \frac{1}{4\varepsilon}\|u\|^2_{\Delta^{-1}}.\end{aligned} \tag{11}$$

Moreover, it holds

$$\|v\|_{\Delta^{-1}} \ge \|v\|_{1,\Omega}, \quad v \in W^{1,2}(\Omega).$$

In view of (8b) and (10) it follows that for $v \in W^{1,2}(\Omega)$ it holds

$$\begin{aligned}&\left\langle \frac{\delta F}{\delta c}, v\right\rangle_{W^{1,2}(\Omega)^*, W^{1,2}(\Omega)}\\ &\quad = -M_c\,(\nabla\mu(c), \nabla v)_{0,\Omega} = (\Delta^{-1}\frac{\partial c}{\partial t}, v)_{0,\Omega}\\ &\quad = -\left(\nabla\Delta^{-1}\frac{\partial c}{\partial t}, \nabla\Delta^{-1}v\right)_{0,\Omega} = -\left(\frac{\partial c}{\partial t}, v\right)_{\Delta^{-1}},\end{aligned}$$

i.e., in this setting $\frac{\partial c}{\partial t}$ is the steepest descent of the free energy functional F.

3 Discretization in time and the splitting scheme

We perform a discretization in time with respect to a partition of the time interval $[0, t_F]$ into subintervals $[t_{m-1}, t_m]$, $1 \le m \le M$, $M \in \mathbb{N}$, of length $\tau_m := t_m - t_{m-1}$. We set $V := BV(\Omega; \omega(\phi^{m-1}))$ and assume that $\Theta^{m-1} \in BV(\Omega; \omega(\phi^{m-2}))$, $\phi^{m-1} \in W^{1,2}(\Omega)$, and $c^{m-1} \in W^{1,2}(\Omega)$ are given.

We introduce the energy functional

$$\begin{aligned}F_1^{m,\tau_m}(\Theta) &:= \frac{1}{2}\|\Theta - \Theta^{m-1}\|^2_{0,\Omega}\\ &\quad + M_\Theta\tau_m\, F_{1,1}(\phi^{m-1}, \Theta) + M_\Theta\tau_m\, F_{1,2}(\phi^{m-1}, \Theta),\\ F_{1,1}(\phi^{m-1}, \Theta) &:= HT\ \mathrm{var}^{\kappa_\Theta}_{\omega(\phi^{m-1})}\,\Theta(\Omega),\\ F_{1,2}(\phi^{m-1}, \Theta)&\\ &:= \frac{\varepsilon_\phi^2 T}{2}\int_\Omega \left(s(\nabla\phi^{m-1}, \Theta)^2|\nabla\phi^{m-1}|^2 + g(\phi^{m-1})\right)dx,\end{aligned}$$

where $\mathrm{var}^{\kappa_\Theta}_{\omega(\phi^{m-1})}\,\Theta(\Omega)$ is the regularized weighted total variation as given by (5).

We define $\Theta^m \in V$ as the minimizer of F_1^{m,τ_m} according to

$$F_1^{m,\tau_m}(\Theta^m) = \inf_{\Theta\in V} F_1^{m,\tau_m}(\Theta). \tag{12}$$

Lemma 3.1 *The energy functional F_1^{m,τ_m} is coercive on V.*

Proof We have

$$\frac{1}{2}\|\Theta - \Theta^{m-1}\|^2_{0,\Omega} \ge \frac{1}{4}\|\Theta\|^2_{0,\Omega} - \frac{1}{2}\|\Theta^{m-1}\|^2_{0,\Omega}. \tag{13}$$

Moreover, observing (4), we get

$$\begin{aligned}&HTM_\Theta\tau_m\int_\Omega s(\nabla\phi^{m-1}, \Theta)^2|\nabla\phi^{m-1}|^2\,dx\\ &\quad \ge HTM_\Theta(1-s_0)^2\tau_m\|\nabla\phi^{m-1}\|^2_{0,\Omega}.\end{aligned} \tag{14}$$

Combining (13) and (14) gives

$$\begin{aligned}F_1^{m,\tau_m}(\Theta) &\ge \frac{1}{4}\|\Theta\|^2_{0,\Omega} + HTM_\Theta\tau_m\ \mathrm{var}^{(\kappa_\Theta)}_{\omega(\phi^{m-1})}\Theta(\Omega)\\ &\quad + HTM_\Theta(1-s_0)^2\tau_m\|\nabla\phi^{m-1}\|^2_{0,\Omega}\\ &\quad + HTM_\Theta\tau_m\int_\Omega g(\phi^{m-1})dx - \frac{1}{2}\|\Theta^{m-1}\|^2_{0,\Omega},\end{aligned} \tag{15}$$

from which we conclude, observing $BV(\Omega; \omega(\phi^{m-1})) \subset L^2(\Omega; \omega(\phi^{m-1})) \subset L^2(\Omega)$ and

$$\mathrm{var}^{(\kappa_\Theta)}_{\omega(\phi^{m-1})}\Theta(\Omega) \ge \mathrm{var}_{\omega(\phi^{m-1})}\Theta(\Omega).$$

□

The functional $F_{1,2}(\phi^{m-1}, \Theta)$ is not convex in Θ in contrast to the remaining part of F_1^{m,τ_m} as given by

$$F_{1,1}^{m,\tau_m}(\Theta) := \frac{1}{2}\|\Theta - \Theta^{m-1}\|^2_{0,\Omega} + M_\Theta\tau_m\ F_{1,1}(\phi^{m-1}, \Theta).$$

Lemma 3.2 *The energy functional $F_{1,1}^{m,\tau_m}$ has the following semicontinuity property: If $\Theta_n \in V, n \in \mathbb{N}$, and $\Theta^m \in V$ such that*

$$\Theta_n \to \Theta^m\ (\mathbb{N} \ni N \to \infty)\ \textit{in}\ L^q(\Omega, \omega(\phi^{m-1})),\ 1 \le q < 2,$$

then it holds

$$var^{(\kappa_\Theta)}_{\omega(\phi^{m-1})}\Theta^m(\Omega) \le \lim\inf_{\mathbb{N}\ni n\to\infty} var^{(\kappa_\Theta)}_{\omega(\phi^{m-1})}\Theta_n(\Omega). \tag{16}$$

Proof We refer to Theorem 3.2 in [4]. □

Theorem 3.1 *The unconstrained minimization problem (12) has a solution $\Theta^m \in V$.*

Proof To prove the existence of a local minimizer, let $(\Theta_n)_{n\in\mathbb{N}}$, $\Theta_n \in V$, $n \in \mathbb{N}$, be a minimizing sequence. Due to the coercivity of $F_{1,1}^{m,\tau_m}$, the sequence is bounded and hence, there exist $\mathbb{N}' \subset \mathbb{N}$ and $\Theta^m \in V$ such that for $\mathbb{N}' \ni n \to \infty$ it holds (cf. Theorem 5.1 in [4])

$$\Theta_n \to \Theta^m \text{ in } L^q(\Omega, \omega(\phi^{m-1})),\ 1 \le q < 2, \tag{17a}$$

$$\Theta_n \rightharpoonup \Theta^m \text{ in } L^2(\Omega). \tag{17b}$$

In view of (17a) we have (16). Further, it follows from (17b) that

$$\|\Theta^m - \Theta^{m-1}\|_{0,\Omega}^2 \le \liminf_{\mathbb{N}'\ni n\to\infty} \|\Theta_n - \Theta^{m-1}\|_{0,\Omega}^2. \tag{18}$$

Due to the continuity of s we also have

$$s(\nabla\phi^{m-1}, \Theta_n)^2 \to s(\nabla\phi^{m-1}, \Theta^m)^2$$

almost everywhere in Ω as $\mathbb{N}' \ni n \to \infty$.
Moreover, the sequence $\{s(\nabla\phi^{m-1}, \Theta_n)^2|\nabla\phi^{m-1}|^2\}_{n\in\mathbb{N}'}$ is uniformly integrable and $s(\nabla\phi^{m-1}, \Theta^m)^2|\nabla\phi^{m-1}|^2 \in L^1(\Omega)$. The Vitali convergence theorem (cf., e.g., [44]) yields

$$F_{1,2}\left(\Theta^m, \phi^{m-1}\right) = \lim_{\mathbb{N}'\ni n\to\infty} F_{1,2}\left(\Theta_n, \phi^{m-1}\right). \tag{19}$$

Hence, (16), (18), and (19) imply

$$F_1^{m,\tau_m}(\Theta^m) \le \liminf_{n\to\infty} F_1^{m,\tau_m}(\Theta_n), \tag{20}$$

which allows to conclude. □

The necessary optimality conditions for (12) are given as follows:

$$\begin{aligned} 0 \in\ & \Theta^m - \Theta^{m-1} + M_\Theta \tau_m (F_{1,2})'(\phi^{m-1}, \Theta^m) \\ & + M_\Theta \tau_m\, \partial F_{1,2}(\phi^{m-1}, \Theta^m), \end{aligned}$$

where $(F_{1,2})'(\phi^{m-1}, \Theta^m)$ is the Gâteaux derivative of $F_{1,2}(\phi^{m-1}, \cdot)$ at Θ^m and $\partial F_{1,1}(\phi^{m-1}, \Theta^m)$ is the subdifferential of $F_{1,1}(\phi^{m-1}, \cdot)$ at Θ^m in the sense of convex analysis. According to [2] we have

$$\begin{aligned} &\partial F_{1,1}(\phi^{m-1}, \Theta^m) = \{-\nabla\cdot\mathbf{z} \mid \mathbf{z} \in H(\mathrm{div}, \Omega), \\ &\mathbf{z} = HT(\kappa_\Theta + |\nabla\Theta^m|^2)^{-1/2}\nabla\Theta^m \\ &\text{almost everywhere in } \Omega,\ \mathbf{n}_\Gamma \cdot \mathbf{z} = 0 \text{ on } \Gamma\}. \end{aligned}$$

The weak formulation amounts to the computation of $\Theta^m \in W^{1,1}(\Omega) \subset V$ such that for all $v_1 \in W^{1,1}(\Omega) \cap L^\infty(\Omega)$ it holds

$$\begin{aligned} &(\Theta^m - \Theta^{m-1}, v_1)_{0,\Omega} + M_\Theta HT\tau_m \int_\Omega \omega(\phi^{m-1}) \\ &\quad (\kappa_\Theta + |\nabla\Theta^m|^2)^{-1/2}\nabla\Theta^m \cdot \nabla v_1\, dx \\ &\quad + M_\Theta \varepsilon_\phi^2 T\tau_m \int_\Omega z(\phi^{m-1}, \Theta^m)|\nabla\phi^{m-1}|^2 v_1\, dx = 0. \end{aligned} \tag{21}$$

Next, with $\Theta^m \in V$ from Theorem 3.1, we consider the energy functional

$$\begin{aligned} &F_2^{m,\tau_m}(\phi) \\ &\quad := \frac{1}{2}\|\phi - \phi^{m-1}\|_{0,\Omega}^2 + M_\phi\tau_m F_2(\phi, c^{m-1}, \Theta^m), \\ &F_2(\phi, c^{m-1}, \Theta^m) \\ &\quad := \int_\Omega \Big(\frac{\varepsilon_\phi^2 T}{2}\, s(\nabla\phi, \Theta^m)^2\, |\nabla\phi|^2 \\ &\qquad + w(c^{m-1})Tg(\phi) + \omega(\phi)(f_S(c^{m-1}, T) + HT\ (\kappa_\Theta \\ &\qquad + HT\ (\kappa_\Theta + |\nabla\Theta^m|^2)^{1/2} \\ &\qquad + (1-\omega(\phi))\, f_L(c^{m-1}, T)\Big)\, dx. \end{aligned}$$

We define $\phi^m \in W^{1,2}(\Omega)$ as the minimizer of F_2^{m,τ_m} according to

$$F_2^{m,\tau_m}(\phi^m) = \inf_{\phi\in W^{1,2}(\Omega)} F_2^{m,\tau_m}(\phi). \tag{22}$$

Lemma 3.3 *The functional F_2^{m,τ_m} is coercive on $W^{1,2}(\Omega)$.*

Proof By Young's inequality we find

$$\frac{1}{2}\|\phi - \phi^{m-1}\|_{0,\Omega}^2 \ge \frac{1}{4}\|\phi\|_{0,\Omega}^2 - \frac{1}{2}\|\phi^{m-1}\|_{0,\Omega}^2.$$

Further, we use the splitting (3) of $f_S(c, T)$ and take advantage of (7) to conclude

$$\begin{aligned} F_2^{m,\tau_m}(\phi) \ge\ & M_\phi \frac{\varepsilon_\phi T}{2}(1-s_0)^2\tau_m\|\nabla\phi\|_{0,\Omega}^2 + \frac{1}{4}\|\phi\|_{0,\Omega}^2 \\ & - (1-\varepsilon_r)M_\phi a\frac{W_S}{4}\tau_m\|c^{m-1}\|_{0,\Omega}^2 - \frac{1}{2}\|\phi^{m-1}\|_{0,\Omega}^2. \end{aligned} \tag{23}$$

The coercivity is an immediate consequence of (23). □

The functional F_2^{m,τ_m} is not convex in ϕ, but it can be split into a convex part $F_{2,1}^{m,\tau_m}$ and non-convex part $F_{2,2}^{m,\tau_m}$ according to

$$\begin{aligned} &F_{2,1}^{m,\tau_m}(\phi) \\ &\quad := \frac{1}{2}\|\phi - \phi^{m-1}\|_{0,\Omega}^2 \\ &\qquad + M_\phi\frac{\varepsilon_\phi T}{2}\tau_m\int_\Omega s(\nabla\phi, \Theta^m)^2|\nabla\phi|^2\, dx, \end{aligned}$$

$$F_{2,2}^{m,\tau_m}(\phi) := M_\phi \tau_m \int_\Omega \Big(w(c^{m-1}) T g(\phi) + \omega(\phi)(f_S(c^{m-1}, T) + HT(\kappa_\Theta + |\nabla \Theta^m|^2)^{1/2} + (1-\omega(\phi)) f_L(c^{m-1}, T) \Big) dx.$$

Lemma 3.4 *For a sufficiently small index of anisotropy $s_0 > 0$ the functional $F_{2,1}^{m,\tau_m}$ is convex in ϕ.*

Proof The convexity of the first part $\|\phi - \phi^{m-1}\|_{0,\Omega}^2/2$ of $F_{2,1}^{m,\tau_m}$ in ϕ is obvious. In order to prove convexity of the second part, for fixed $\gamma \in \mathbb{R}$ we set

$$g_1(\boldsymbol{\eta}) := (1 - s_0 \cos(m_S \vartheta - 2\pi\gamma)))^2 (\eta_1^2 + \eta_2^2),$$

where $\boldsymbol{\eta} = (\eta_1, \eta_2)$ and ϑ is given by (4). Computing the second partial derivatives $\partial^2 g_1/\partial \eta_i^2$, $1 \le i \le 2$, and $\partial^2 g_1/(\partial\eta_1 \partial\eta_2)$, it can be shown that for sufficiently small s_0 the Hessian of g_1 is positive definite, i.e., there exists $\alpha > 0$ such that

$$\sum_{i,j=1}^{2} \frac{\partial^2 g_1}{\partial \eta_i \partial \eta_j} \xi_i \xi_j \ge \alpha |\xi|^2 \quad \text{for all } \xi = (\xi_1, \xi_2)^T \in \mathbb{R}^2.$$

□

Theorem 3.2 *For a sufficiently small index of anisotropy $s_0 > o$ the unconstrained minimization problem (22) has a solution $\phi^m \in W^{1,2}(\Omega)$.*

Proof Let $\{\phi_n\}_{\mathbb{N}}$, $\phi_n \in W^{1,2}(\Omega)$, be a minimizing sequence, i.e., it holds

$$F_2^{m,\tau_m}(\phi_n) \to \inf_{\phi \in W^{1,2}(\Omega)} F_2^{m,\tau_m}(\phi) \quad (n \to \infty). \tag{24}$$

Due to the coercivity of F_2^{m,τ_m} the sequence $\{\phi_n\}_{\mathbb{N}}$ is bounded in $W^{1,2}(\Omega)$. Hence, there exists a weakly convergent subsequence, i.e., there exist $\mathbb{N}' \subset \mathbb{N}$ and $\phi^m \in W^{1,2}(\Omega)$ such that $\phi_n \rightharpoonup \phi^m$ ($\mathbb{N}' \ni n \to \infty$) in $W^{1,2}(\Omega)$. The Rellich-Kondrachev theorem implies strong convergence in $L^p(\Omega)$ for any $1 \le p < \infty$ and hence, there exists a subsequence $\mathbb{N}'' \subset \mathbb{N}'$ such that

$$\phi_n \to \phi^m \quad \text{almost everywhere in } \Omega \text{ as } \mathbb{N}'' \ni n \to \infty.$$

Setting

$$h(\phi) := w(c^{m-1}) T g(\phi) + \omega(\phi)(f_S(c^{m-1}, T) HT(\kappa_\Theta + |\nabla \Theta^m|^2)^{1/2} + (1-\omega(\phi)) f_L(c^{m-1}, T),$$

the continuity of g, ω, and w implies

$$h(\phi_n) \to h(\phi^m) \text{ a.e. in } \Omega \text{ as } \mathbb{N}'' \ni n \to \infty.$$

Moreover, the sequence $\{h(\phi_n)\}_{\mathbb{N}''}$ is uniformly integrable and $h(\phi^m) \in L^1(\Omega)$. The Vitali convergence theorem gives

$$F_{2,2}^{m,\tau_m}(\phi_n) \to F_{2,2}^{m,\tau_m}(\phi^m) \quad \text{as } \mathbb{N}'' \ni n \to \infty. \tag{25}$$

Obviously, the functional $F_{2,1}^{m,\tau_m}$ is continuous on $W^{1,2}(\Omega)$ and thus lower semicontinuous. Since it is convex according to Lemma 3.4, it is weakly lower semicontinuous which gives

$$F_{2,1}^{m,\tau_m}(\phi^m) \le \liminf_{\mathbb{N}' \ni n \to \infty} F_{2,1}^{m,\tau_m}(\phi_n). \tag{26}$$

Now, (24), (25), and (26) imply that ϕ^m satisfies (22). □

The necessary optimality conditions for the unconstrained minimization problem (22) give rise to the following nonlinear second order elliptic boundary value problem

$$(\phi^m - \phi^{m-1}) - M_\phi \tau_m \Big(\varepsilon_\phi^2 T \nabla \cdot (a(\nabla\phi^m, \Theta^m)\nabla\phi^m) + r(\phi^m, c^{m-1}, \Theta^m) \Big) = 0 \quad \text{in } \Omega,$$
$$\mathbf{n}_\Gamma \cdot a(\phi^m)\nabla\phi^m = 0 \quad \text{on } \Gamma,$$

whose weak solution is: Find $\phi^m \in W^{1,2}(\Omega)$ such that for all $v_2 \in W^{1,2}(\Omega) \cap L^\infty(\Omega)$ it holds

$$(\phi^m - \phi^{m-1}, v_2)_{0,\Omega} + M_\phi \tau_m \Big(\varepsilon_\phi^2 T (a(\nabla\phi^m, \Theta^m)\nabla\phi^m, \nabla v_2)_{0,\Omega} + (r(\phi^m, c^{m-1}, \Theta^m), v_2)_{0,\Omega} \Big) = 0. \tag{27}$$

Given $\Theta^m \in V$ and $\phi^m \in W^{1,2}(\Omega)$ as the solutions of (12) and (22), we finally consider the energy functional

$$F_3^{m,\tau_m}(c) := \frac{1}{2} \|c - c^{m-1}\|_{\Delta^{-1}}^2 + M_c \tau_m F_2(\phi^m, c, \Theta^m),$$
$$F_3(\phi^m, c, \Theta^m) := \int_\Omega \Big(\frac{\varepsilon_c^2 T}{2} |\nabla c|^2 + w(c) T g(\phi^m) + \omega(\phi^m)(f_S(c, T) + (1-\omega(\phi^m)) f_L(c, T) \Big) dx$$

and define $c^m \in W^{1,2}(\Omega)$ as the minimizer of F_3^{m,τ_m} according to

$$F_3^{m,\tau_m}(c^m) = \inf_{c \in W^{1,2}(\Omega)} F_3^{m,\tau_m}(c). \tag{28}$$

Let us assume that the time-step size τ_m satisfies

$$\tau_m < \frac{\varepsilon_c^2 T}{M_c a W_S}. \tag{29}$$

Lemma 3.5 *Under the assumption (29) the functional F_3^{m,τ_m} is coercive on $W^{1,2}(\Omega)$.*

Proof As in the proof of Lemma 3.3 Young's inequality yields

$$\frac{1}{2}\,\|c-c^{m-1}\|_{\Delta^{-1}}^2 \geq \frac{1}{4}\,\|c\|_{\Delta^{-1}}^2 - \frac{1}{2}\,\|c^{m-1}\|_{\Delta^{-1}}^2.$$

Again, we split $f_S(c,T)$ by means of (3) and take advantage of (7) and (11) with $\varepsilon = \varepsilon_c^2 T/4$. We thus obtain

$$F_3^{m,\tau_m}(c) \geq M_c\tau_m \int_\Omega \frac{\varepsilon_c^2 T}{4}|\nabla c|^2\,dx + \Big(\frac{1}{4} - \frac{M_c a W_S}{4\varepsilon_c^2 T}\tau_m\Big)\|c\|_{\Delta^{-1}}^2 - \frac{1}{2}\|c^{m-1}\|_{\Delta^{-1}}^2. \tag{30}$$

Under the assumption (29) the assertion follows from (30). □

Again, the energy functional F_3^{m,τ_m} is split into a convex part $F_{3,1}^{m,\tau_m}$ and a non-convex part $F_{3,2}^{m,\tau_m}$:

$$F_{3,1}^{m,\tau_m}(c) := \frac{1}{2}\,\|c-c^{m-1}\|_{\Delta^{-1}}^2 + M_c\tau_m\int_\Omega \frac{\varepsilon_c^2 T}{2}|\nabla c|^2\,dx,$$

$$F_{3,2}^{m,\tau_m}(c) := M_c\tau_m\int_\Omega \Big(w(c)Tg(\phi^m) + \omega(\phi^m)(f_S(c,T) + (1-\omega(\phi^m))f_L(c,T)\Big)dx.$$

The convexity of $F_{3,1}^{m,\tau_m}$ is obvious.

Theorem 3.3 *Under the assumption* (29) *the unconstrained minimization problem* (28) *has a solution* $c^m \in W^{1,2}(\Omega)$.

Proof Let $\{c_n\}_{\mathbb{N}}$, $c_n \in W^{1,2}(\Omega)$, be a minimizing sequence, i.e., we have

$$F_3^{m,\tau_m}(c_n) \to \inf_{c\in\bar{V}_c} F_3^{m,\tau_m}(c) \quad (n\to\infty). \tag{31}$$

Since $F_3^{m,\Delta t}$ is coercive, the sequence $\{c_n\}_{\mathbb{N}}$ is bounded in $W^{1,2}(\Omega)$. Consequently, there exists a weakly convergent subsequence, i.e., there exist $\mathbb{N}'\subset\mathbb{N}$ and $c^m\in W^{1,2}(\Omega)$ such that $c_n \rightharpoonup c^m$ ($\mathbb{N}'\ni n\to\infty$) in $W^{1,2}(\Omega)$. In view of the Rellich-Kondrachev theorem we have strong convergence in $L^p(\Omega)$ for any $1\leq p<\infty$. It follows that there exists a subsequence $\mathbb{N}''\subset\mathbb{N}'$ such that

$$c_n \to c^m \text{ almost everywhere in } \Omega \text{ as } \mathbb{N}''\ni n\to\infty.$$

Setting $\ell(c) := w(c)Tg(\phi^m) + \omega(\phi^m)(f_S(c,T) + (1-\omega(\phi^m))f_L(c,T)$, the continuity of f_L, f_S, and w implies

$$\ell(c_n)\to\ell(c^m) \text{ almost everywhere in } \Omega \text{ as } \mathbb{N}''\ni n\to\infty.$$

Moreover, the sequence $\{\ell(c_n)\}_{\mathbb{N}''}$ is uniformly integrable and $\ell(c^m)\in L^1(\Omega)$. The Vitali convergence theorem yields

$$F_{3,2}^{m,\tau_m}(c_n) \to F_{3,2}^{m,\tau_m}(c^m) \quad \text{as } \mathbb{N}''\ni n\to\infty. \tag{32}$$

The functional $F_{3,1}^{m,\tau_m}$ is continuous on $W^{1,2}(\Omega)$ and thus lower semicontinuous. Due to its convexity it is weakly lower semicontinuous whence

$$F_{3,1}^{m,\tau_m}(c^m) \leq \liminf_{\mathbb{N}'\ni n\to\infty} F_{3,1}^{m,\tau_m}(c_n). \tag{33}$$

From (31), (32), and (33) we deduce that c^m satisfies (28). □

The necessary optimality conditions for the unconstrained minimization problem (28) lead to the following nonlinear elliptic boundary value problem

$$c^m - c^{m-1} - M_c\tau_m\Delta w^m = 0 \quad \text{in } \Omega, \tag{34a}$$

$$w^m = \mu(\phi^m, c^m), \tag{34b}$$

$$\mathbf{n}_\Gamma\cdot\nabla c^m = 0,\ \mathbf{n}_\Gamma\cdot w^m = 0 \quad \text{on } \Gamma. \tag{34c}$$

The weak formulation of (34a)–(34c) is to find $c^m\in W^{1,2}(\Omega)$, $w^m\in W^{1,2}(\Omega)$ such that for all $v_3\in W^{1,2}(\Omega)$ and $v_4\in W^{1,2}(\Omega)\cap L^\infty(\Omega)$ it holds

$$(c^m - c^{m-1}, v_3)_{0,\Omega} + M_c\tau_m\int_\Omega \nabla w_m\cdot\nabla v_3\,dx = 0, \tag{35a}$$

$$(w^m, v_4)_{0,\Omega} = \varepsilon_c^2 T\int_\Omega \nabla c^m\cdot\nabla v_4\,dx + \int_\Omega h(\phi^m, c^m)v_4\,dx. \tag{35b}$$

4 Discretization in space

Let $\mathcal{T}_h$ be a geometrically conforming, shape-regular, simplicial triangulation of Ω. We denote by $\mathcal{E}_h^\Omega$ and $\mathcal{E}_h^\Gamma$ the set of edges of $\mathcal{T}_h$ in the interior of Ω and on the boundary Γ, respectively, and set $\mathcal{E}_h := \mathcal{E}_h^\Omega\cup\mathcal{E}_h^\Gamma$. For $K\in\mathcal{T}_h$ and $E\in\mathcal{E}_h$ we denote by h_K and h_E the diameter of K and the length of E. Denoting by $P_k(T)$, $k\in\mathbb{N}$, the linear space of polynomials of degree $\leq k$ on T, for $k\geq 2$ we define

$$V_h := \{v_h\in C^0(\bar\Omega)\mid v_h|_K\in P_k(K),\ K\in\mathcal{T}_h\},$$

and note that $V_h\subset H^1(\Omega)$, but $V_h\not\subset H^2(\Omega)$. For interior edges $E\in\mathcal{E}_h^\Omega$ such that $E = K_+\cap K_-$, $K_\pm\in\mathcal{T}_h$ and boundary edges on Γ we introduce the average and jump of ∇v_h according to

$$\{\nabla v_h\}_E := \begin{cases} \frac{1}{2}\Big(\nabla v_h|_{E\cap K_+} + \nabla v_h|_{E\cap K_-}\Big) & E\in\mathcal{E}_h(\Omega) \\ \nabla v_h|_E & E\in\mathcal{E}_h(\Gamma)\end{cases},$$

$$[\nabla v_h]_E := \begin{cases} \nabla v_h|_{E\cap K_+} - \nabla v_h|_{E\cap K_-} & E \in \mathcal{E}_h(\Omega) \\ \nabla v_h|_E & E \in \mathcal{E}_h(\Gamma) \end{cases}.$$

The average $\{\Delta v_h\}_E$ and jump $[\Delta v_h]_E$ are defined analogously. We further denote by $\mathbf{n}_E$ the unit normal vector on E pointing in the direction from K_+ to K_-.

In order to motivate the C^{0}IPDG approximation of the implicitly in time discretized Cahn–Hilliard type equation (35), for $w_h^m \in V_h$ and $u_h^m \in V_h$ we consider (34a), (34b) elementwise, i.e.,

$$w_h^m = -\varepsilon_c^2 T \Delta c_h^m + h(\phi_h^m, c_h^m), \tag{36a}$$

$$c_h^m - c_h^{m-1} = M_c \tau_m \Delta w_h^m \quad \text{in } K \in \mathcal{T}_h(\Omega). \tag{36b}$$

We multiply (36a) by $z_h \in W_h := \{w_h \in L^2(\Omega) \mid w_h|_K \in P_k(K),\ K \in \mathcal{T}_h(\Omega)\}$ and integrate over K:

$$\int_K w_h^m z_h \, dx = -\varepsilon_c^2 T \int_K \Delta c_h^m z_h \, dx + \int_K h(\phi_h^m, c_h^m) z_h \, dx. \tag{37}$$

An application of Green's formula yields

$$\int_K \Delta c_h^m z_h \, dx = -\int_K \nabla c_h^m \cdot \nabla z_h \, dx + \int_{\partial K} \mathbf{n}_{\partial K} \cdot \nabla c_h^m z_h \, ds. \tag{38}$$

On the other hand, multiplying (36b) by $v_h \in V_h$ and integrating over K gives

$$\int_K \left(c_h^m - c_h^{m-1}\right) v_h \, dx = M_c \tau_m \int_K \Delta w_h^m v_h \, dx. \tag{39}$$

By another application of Green's formula we obtain

$$\int_K \Delta w_h^m v_h \, dx = \int_K w_h^m \Delta v_h \, dx + \int_{\partial K} \mathbf{n}_{\partial K} \cdot \nabla w_h^m v_h \, ds - \int_{\partial K} w_h^m \mathbf{n}_{\partial K} \cdot \nabla v_h \, ds. \tag{40}$$

It follows from (37)–(40) that

$$\int_K w_h^m z_h \, dx = \varepsilon_c^2 T \left(\int_K \nabla c_h^m \cdot \nabla z_h \, dx - \int_{\partial K} \mathbf{n}_{\partial K} \cdot \nabla c_h^m z_h \, ds \right) + \int_K h(\phi_h^m, c_h^m) z_h \, dx, \tag{41a}$$

$$\int_K \left(c_h^m - c_h^{m-1}\right) v_h \, dx = M_c \tau_m \left(\int_K w_h^m \Delta v_h \, dx + \int_{\partial K} \mathbf{n}_{\partial K} \cdot \nabla w_h^m v_h \, ds - \int_{\partial K} w_h^m \mathbf{n}_{\partial K} \cdot \nabla v_h \, ds \right). \tag{41b}$$

Summing over all $K \in \mathcal{T}_h$ in (41a) and (41b), we obtain the weak formulation of the mixed formulation (36a), (36b). A general C^{0}DG approximation is based on the weak formulation of the mixed formulation and characterized by numerical flux functions $\hat{\mathbf{c}}_{\partial K}^m$ and $\hat{w}_{\partial K}^m$. We are looking for a pair $(c_h^m, w_h^m) \in V_h \times W_h$ such that for all $(v_h, z_h) \in V_h \times W_h$ it holds

$$\sum_{K\in\mathcal{T}_h(\Omega)} \int_K w_h^m z_h \, dx = \varepsilon_c^2 T \sum_{K\in\mathcal{T}_h(\Omega)} \left(\int_K \nabla c_h^m \cdot \nabla z_h \, dx - \int_{\partial K} \mathbf{n}_{\partial K} \cdot \hat{\mathbf{c}}_{\partial K}^m z_h \, ds \right) + \sum_{K\in\mathcal{T}_h(\Omega)} \int_K h(\phi_h^m, c_h^m) z_h \, dx, \tag{42a}$$

$$\sum_{K\in\mathcal{T}_h(\Omega)} \int_K \left(c_h^m - c_h^{m-1}\right) v_h \, dx = M_c \tau_m \sum_{K\in\mathcal{T}_h(\Omega)} \left(\int_K w_h^m \Delta v_h \, dx - \int_{\partial K} \hat{w}_{\partial K}^m \mathbf{n}_{\partial K} \cdot \nabla v_h \, ds \right). \tag{42b}$$

In particular, for the C^{0}IPDG approximation the numerical flux functions $\hat{\mathbf{c}}_{\partial K}^m$ and $\hat{w}_{\partial K}^m$ are given by

$$\hat{\mathbf{c}}_{\partial K}^m|_E := \begin{cases} \{\nabla c_h^m\}_E & E \in \mathcal{E}_h^\Omega \\ \mathbf{0} & E \in \mathcal{E}_h^\Gamma \end{cases}, \tag{43a}$$

$$\hat{w}_{\partial K}^m := \varepsilon_c^2 T \left(\{\Delta u_h^m\}_E - \alpha h_E^{-1} \mathbf{n}_E \cdot [\nabla c_h^m]_E \right), \tag{43b}$$

where $\alpha > 0$ is a penalty parameter. This particular choice of the numerical flux functions allows to eliminate w_h^m from the system (42a), (42b). In fact, if we choose $z_h = \Delta v_h$ in (42a), we obtain the following C^{0}IPDG approximation of the implicitly in time discretized Cahn–Hilliard type equation for the concentration field:

Find $c_h^m \in V_h$ such that for all $v_h \in V_h$ it holds

$$\left(c_h^m, v_h\right)_{0,\Omega} + \tau_m \, a_h^{DG}\left(c_h^m, v_h\right) = \left(c_h^{m-1}, v_h\right)_{0,\Omega}, \tag{44}$$

where the C^{0}IPDG semilinear form $a_h^{DG}(\cdot,\cdot)$ is given by

$$a_h^{DG}(c_h, v_h) := M_c \sum_{K\in\mathcal{T}_h(\Omega)} \left(\varepsilon_c^2 T \int_K \Delta c_h \Delta v_h \, dx + \int_K h(\phi_h^m, c_h) \Delta v_h \, dx \right)$$

$$
\begin{aligned}
&- M_c \varepsilon_c^2 T \sum_{E \in \mathcal{E}_h(\bar{\Omega})} \int_E \Big(\{\Delta c_h\}_E \, \mathbf{n}_E \cdot [\nabla v_h]_E \, ds \\
&- M_c \varepsilon_c^2 T \sum_{E \in \mathcal{E}_h(\bar{\Omega})} \mathbf{n}_E \cdot [\nabla c_h]_E \{\Delta v_h\}_E \Big) \, ds \\
&+ \alpha M_c \varepsilon_c^2 T \sum_{E \in \mathcal{E}_h(\bar{\Omega})} h_E^{-1} \int_E \mathbf{n}_E \cdot [\nabla c_h]_E \, \mathbf{n}_E \cdot [\nabla v_h]_E \, ds.
\end{aligned} \tag{45}
$$

The advantage of the C^0IPDG approximation is that the finite element space V_h can be used as well for the spatial discretization of the implicitly in time discretized equations (21) for the orientation angle and (27) for the local degree of crystallinity. In particular, for the former one we are looking for $\Theta_h^m \in V_h$ such that

$$
\begin{aligned}
&(\Theta_h^m, v_h)_{0,\Omega} \\
&\quad + M_\Theta H T \tau_m (\omega(\phi_h^{m-1})(\kappa_\Theta + |\nabla \Theta_h^m|^2)^{-1/2} \nabla \Theta_h^m, \nabla v_h)_{0,\Omega} \\
&\quad + M_\Theta \varepsilon_\phi^2 T \tau_m (z(\phi_h^{m-1}, \Theta_h^m) |\nabla \phi_h^{m-1}|^2, v_h)_{0,\Omega} \\
&= (\Theta_h^{m-1}, v_h)_{0,\Omega}, \quad v_h \in V_h.
\end{aligned} \tag{46}
$$

On the other hand, the latter one amounts to the computation of $\phi_h^m \in V_h$ such that

$$
\begin{aligned}
&(\phi_h^m, v_h)_{0,\Omega} + M_\phi \tau_m \Big(\varepsilon_\phi^2 T (a(\nabla \phi_h^m, \Theta_h^m) \nabla \phi_h^m, \nabla v_h)_{0,\Omega} \\
&\quad + (r(\phi_h^m, c_h^{m-1}, \Theta_h^m), v_h)_{0,\Omega} \Big) \\
&= (\phi_h^{m-1}, v_h)_{0,\Omega}, \quad v_h \in V_h.
\end{aligned} \tag{47}
$$

The existence of solutions Θ_h^m, ϕ_h^m, and c_h^m of the fully discretized equations (46), (47), and (44) can be shown in a similar way as in the previous section.

Remark 4.1 The regularization parameter κ_Θ should be chosen according to $\kappa_\Theta = O(h)$ in order to obtain the same qualitative approximation properties as for the unregularized problem (cf.,e.g., [5]).

5 Predictor corrector continuation strategy

The numerical solution of (44), (46), and (47) amounts to the successive solution of three nonlinear algebraic systems. We assume $V_h = \mathrm{span}\{\varphi_1, \ldots, \varphi_{N_h}\}$, $N_h \in \mathbb{N}$, such that

$$
\Theta_h^m = \sum_{j=1}^{N_h} x_{1,j}^m \varphi_j, \;\; \phi_h^m = \sum_{j=1}^{N_h} x_{2,j}^m \varphi_j, \;\; c_h^m = \sum_{j=1}^{N_h} x_{3,j}^m \varphi_j.
$$

Setting

$$
\mathbf{x}_i^m = \left(x_{i,1}^m, \ldots, x_{i,N_h}^m \right)^T, \;\; 1 \le i \le 3,
$$

the algebraic formulation of (44), (46), and (47) leads to the three nonlinear systems

$$
\mathbf{F}_k \left(\mathbf{x}_k^m, t_m \right) = \mathbf{0}, \quad 1 \le k \le 3, \tag{48}
$$

where $\mathbf{F}_k : \mathbb{R}^{N_h} \times \mathbb{R}^{N_h} \times \mathbb{R}_+ \to \mathbb{R}^{N_h}$, $1 \le k \le 3$, and the components $\mathbf{F}_{k,i}$, $1 \le i \le N_h$, are given by

$$
\begin{aligned}
\mathbf{F}_{1,i}(\mathbf{x}_1^m, t_m) &:= \sum_{j=1}^{N_h} x_{1,j}^m (\varphi_j, \varphi_i)_{0,\Omega} \\
&\quad + M_\Theta H T \tau_m \sum_{j=1}^{N_h} x_{1,j}^m \left(\omega(\mathbf{x}_2^{m-1}) b(\mathbf{x}_1^m) \nabla \varphi_j, \nabla \varphi_i \right)_{0,\Omega} \\
&\quad + M_\Theta \varepsilon_\phi^2 T \tau_m \left(z\left(\mathbf{x}_2^{m-1}, \mathbf{x}_1^m \right) | \sum_{k=1}^{N_h} x_{2,k}^{m-1} \nabla \varphi_k |^2, \varphi_i \right)_{0,\Omega} \\
&\quad - \sum_{j=1}^{N_h} x_{1,j}^{m-1} (\varphi_j, \varphi_i)_{0,\Omega}, \\
\mathbf{F}_{2,i}(\mathbf{x}_2^m, t_m) &:= \sum_{j=1}^{N_h} x_{2,j}^m (\varphi_j, \varphi_i)_{0,\Omega} \\
&\quad + M_\phi \tau_m \Big(\varepsilon_\phi^2 T \sum_{j=1}^{N_h} x_{2,j}^m \left(a\left(\mathbf{x}_2^m, \mathbf{x}_1^m \right) \nabla \varphi_j, \nabla \varphi_i \right)_{0,\Omega} \\
&\quad + \left(r\left(\mathbf{x}_2^m, \mathbf{x}_3^{m-1}, \mathbf{x}_1^m \right), \varphi_i \right)_{0,\Omega} \Big) - \sum_{j=1}^{N_h} x_{2,j}^{m-1} (\varphi_j, \varphi_i)_{0,\Omega}, \\
\mathbf{F}_{3,i}(\mathbf{x}_3^m, t_m) &:= \sum_{j=1}^{N_h} x_{3,j}^m (\varphi_j, \varphi_i)_{0,\Omega} \\
&\quad + \tau_m \, a_h^{DG} \left(\sum_{j=1}^{N_h} x_{3,j}^m \varphi_j, \varphi_i \right) - \sum_{j=1}^{N_h} x_{3,j}^m (\varphi_j, \varphi_i)_{0,\Omega}.
\end{aligned}
$$

where

$$
\begin{aligned}
z\left(\mathbf{x}_{2,}^{m-1}, \mathbf{x}_1^m \right) &:= z\left(\sum_{k=1}^{N_h} x_{2,k}^{m-1} \varphi_k, \sum_{k=1}^{N_h} x_{1,k}^m \varphi_k \right), \\
b\left(\mathbf{x}_1^m \right) &:= (\kappa_\Theta + | \sum_{k=1}^{N_h} x_{1,k}^m \nabla \varphi_k |^2)^{-1/2}, \\
a\left(\mathbf{x}_2^m, \mathbf{x}_1^m \right) &:= a\left(\sum_{k=1}^{N_h} x_{2,k}^m \nabla \varphi_k, \sum_{k=1}^{N_h} x_{1,k}^m \varphi_k \right), \\
r\left(\mathbf{x}_2^m, \mathbf{x}_3^{m-1}, \mathbf{x}_1^m \right) &:= r\left(\sum_{k=1}^{N_h} x_{2,k}^m \varphi_k, \sum_{k=1}^{N_h} x_{3,k}^{m-1} \varphi_k, \sum_{k=1}^{N_h} x_{1,k}^m \varphi_k \right).
\end{aligned}
$$

The nonlinear systems (48) can be solved by Newton's method, but the problem is the appropriate choice of the

time step sizes $\tau_m, 1 \le m \le M$, in order to guarantee convergence of Newton's method. In fact, a uniform choice $\tau_m = T/M$ only works, if M is chosen sufficiently large which would require an unnecessary huge amount of time steps. In particular, this applies to the nonlinear system (48) for $k = 1$ reflecting the singular character of the second order total variation flow problem. An appropriate way to overcome this difficulty is to apply a predictor corrector continuation strategy with an adaptive choice of the time steps (cf., e.g., [16,30]). Given the triple $(\mathbf{x}_1^{m-1}, \mathbf{x}_2^{m-1}, \mathbf{x}_3^{m-1})$, the time step size $\tau_{m-1,0} = \tau_{m-1}$, and setting $k = 0$, where k is a counter for the predictor corrector steps, the predictor step for (48) consists of constant continuation leading to the initial guesses

$$\mathbf{x}_i^{(m,k)} = \mathbf{x}_i^{m-1}, \ 1 \le i \le 3, \ t_m = t_{m-1} + \tau_{m-1,k}. \tag{49}$$

We set $i = 1$, where $1 \le i \le 3$ is a counter for the nonlinear system. Setting further $\nu_i = 0$ as well as $\mathbf{x}_i^{(m,k,\nu_i)} = \mathbf{x}_i^{(m,k)}$, for $\nu_i \le \nu_{max}$, where $\nu_{max} > 0$ is a pre-specified maximal number, the Newton iteration

$$\begin{aligned} &\mathbf{F}_i'(\mathbf{x}_i^{(m,k,\nu_i)}, t_m)\boldsymbol{\Delta}\mathbf{x}_i^{(m,k,\nu_i)} = -\mathbf{F}_i(\mathbf{x}_i^{(m,k,\nu_i)}, t_m), \\ &\mathbf{x}_i^{(m,k,\nu_i+1)} = \mathbf{x}_i^{(m,k,\nu_i)} + \boldsymbol{\Delta}\mathbf{x}_i^{(m,k,\nu_i)}, \quad \nu_i \ge 0, \end{aligned} \tag{50}$$

serves as a corrector whose convergence is monitored by the contraction factor

$$\Lambda_{\mathbf{x}_i}^{(m,k,\nu_i)} = \frac{\|\overline{\boldsymbol{\Delta}\mathbf{x}_i^{(m,k,\nu_i)}}\|}{\|\boldsymbol{\Delta}\mathbf{x}_i^{(m,k,\nu_i)}\|}, \tag{51}$$

where $\overline{\boldsymbol{\Delta}\mathbf{x}_i^{(m,k,\nu_i)}}$ is the solution of the auxiliary Newton step

$$\mathbf{F}_1'\left(\mathbf{x}_i^{(m,k,\nu_i)}, t_m\right)\overline{\boldsymbol{\Delta}\mathbf{x}_i^{(m,k,\nu_i)}} = -\mathbf{F}_1\left(\mathbf{x}_i^{(m,k,\nu_i+1)}, t_m\right). \tag{52}$$

If the contraction factor satisfies

$$\Lambda_{\mathbf{x}_1}^{(m,k,\nu_i)} < \frac{1}{2}, \tag{53}$$

we set $\nu_i = \nu_i + 1$. If $\nu_i > \nu_{max}$, both the Newton iteration and the predictor corrector continuation strategy are terminated indicating non-convergence. Otherwise, we continue the Newton iteration (50). If (53) does not hold true, we set $k = k + 1$ and the time step is reduced according to

$$\tau_{m,k} = \max\left(\frac{\sqrt{2}-1}{\sqrt{4\Lambda_{\mathbf{x}_i}^{(m,k,\nu_i)} + 1} - 1}\,\tau_{m,k-1}, \tau_{min}\right), \tag{54}$$

where $\tau_{min} > 0$ is some pre-specified minimal time step. If $\tau_{m,k} \ge \tau_{min}$, we set $i = 1$ and go back to the prediction step (49). Otherwise, the predictor corrector strategy is stopped indicating non-convergence. The Newton iteration is terminated successfully, if for some $\nu_i^* > 0$ the relative error of two subsequent Newton iterates satisfies

$$\frac{\|\mathbf{x}_i^{(m,k,\nu_i^*)} - \mathbf{x}_i^{(m,k,\nu_i^*-1)}\|}{\|\mathbf{x}_i^{(m,k,\nu_i^*)}\|} < \varepsilon \tag{55}$$

for some pre-specified accuracy $\varepsilon > 0$. In this case, we set $i = i + 1$. As long as $i \le 3$, we continue with the Newton iteration for the next nonlinear system. If $i > 3$, we set

$$\mathbf{x}_i^m = \mathbf{x}_i^{(m,k,\nu_i^*)}, \quad 1 \le i \le 3, \tag{56}$$

and predict a new time step according to

$$\tau_m = \min\left(\min_{1\le i\le 3} \frac{(\sqrt{2}-1)\,\|\boldsymbol{\Delta}\mathbf{x}_i^{(m,k,0)}\|}{2\Lambda_{\mathbf{x}_i}^{(m,k,0)}\,\|\mathbf{x}_i^{(m,k,0)} - \mathbf{x}_i^m\|}, \text{amp}\right)\tau_{m,k}, \tag{57}$$

where amp > 1 is a pre-specified amplification factor for the time step sizes. We set $m = m + 1$ and begin new predictor corrector iterations for the time interval $[t_m, t_{m+1}]$.

6 Numerical results

We have applied the splitting scheme to two examples, namely the crystallization of a single crystal (Example 1) and the crystallization of four single crystals with different orientation angles (Example 2). In both examples the physical domain has been $\Omega = (0.8\ \mu\text{m}, 0.8\ \mu\text{m})^2$, and we have chosen the same physical data, i.e., interface free energy constants, temperature and mobilities, constants for the Helmholtz free energy, and constants for the anisotropy function s and the functions w and ω as displayed in Tables 1, 2, 3, 4 and 5.

For the finite element approximation we have chosen a uniform grid of mesh width h, polynomial degree k, penalty parameter α for the C^0IPDG approximation of the Cahn–Hilliard type equation, and regularization parameter κ_Θ for the regularization of the second order total variation flow problem as shown in Table 6. The parameters for the predictor corrector continuation strategy are given in Table 7.

Table 1 Physical data: interface free energy constants

ε_ϕ	ε_c	H
3.0×10^{-11}	4.0×10^{-13}	1.0×10^{-3}

Table 2 Physical data: temperature and mobilities

T	M_Θ	M_ϕ	M_c
298.15	1.0	1.0×10^4	1.0×10^{-4}

Table 3 Physical data for the Helmholtz free energy I

W_L	β_L	$T_M^{(L)}$
4.0	9.15×10^{-2}	273.15

Table 4 Physical data for the Helmholtz free energy II

W_S	β_S	$T_M^{(S)}$
4.0	-1.31×10^{-1}	343.15

Table 5 Physical data: Anisotropy function s, function w, and function ω

s_0	m_s	w_L	w_S	ε_w	ε_r
0.04	4	0.5	0.05	1.0×10^{-3}	1.0×10^{-3}

Table 6 Computational data for the C^0IPDG approximation: mesh width, polynomial degree, penalization parameter, and regularization parameter

h	k	α	κ_Θ
8.8×10^{-2} µm	2	12.5	1.0×10^{-3}

Table 7 Computational data for the predictor corrector continuation strategy: maximum number of Newton iterations, minimum time step size, relative accuracy of Newton iterations, and amplification factor for new time step size

ν_{max}	τ_{min}	ε	amp
50	1.0×10^{-6}	1.0×10^{-3}	1.2

Example 1 We consider the growth of a single crystal which is initially occupying a subdomain Ω_0 around the center of the computational domain Ω. The initial data are given by

$$\Theta_h^0 = \begin{cases} 1.2\,\pi & x \in \bar{\Omega}_0 \\ 1.0 \pm 0.05\,\pi & \text{elsewhere} \end{cases},$$

$$\phi_h^0 = \begin{cases} 1.0 & x \in \bar{\Omega}_0 \\ 0.0 & \text{elsewhere} \end{cases},$$

$$c_h^0 = \begin{cases} 1.0 & x \in \bar{\Omega}_0 \\ 0.5 \pm 0.05 & \text{elsewhere} \end{cases},$$

where the values for Θ_h^0 and c_h^0 outside Ω_0 are chosen randomly.

The initial configuration for Θ_h and ϕ_h is shown in Fig. 1 (left), whereas Fig. 1 (middle) and Fig. 1 (right) display the values at the intermediate time $t = 2.07 \times 10^{-2}$ and the time $t = 1.38 \cdot 10^{-1}$. For Θ_h 'red' represents the orientation angle $1.2\,\pi$ and for ϕ_h 'red' and 'blue' represent the local degrees of crystallinity 1.0 and 0.0, respectively. We see that the crystal grows in time with a narrow interface featuring steep gradients, in particular for the orientation angle which is typical for second order total variation flow problems.

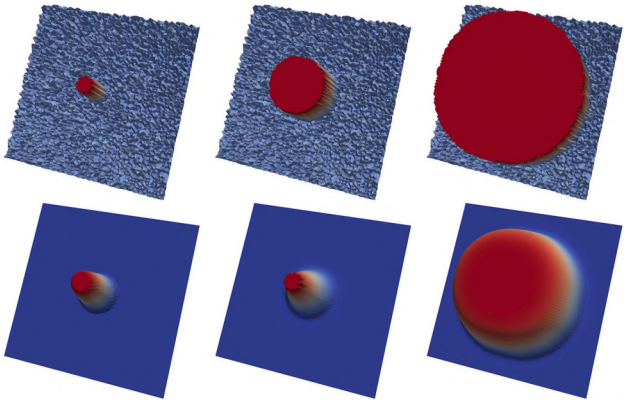

Fig. 1 Example 1: Anisotropic growth of a crystal. Orientation angle (top) and local degree of crystallinity (bottom) at initial time $t = 0$ s (left), at time $t = 2.07 \times 10^{-2}$ s (middle), and at time $t = 1.38 \times 10^{-1}$ s (right)

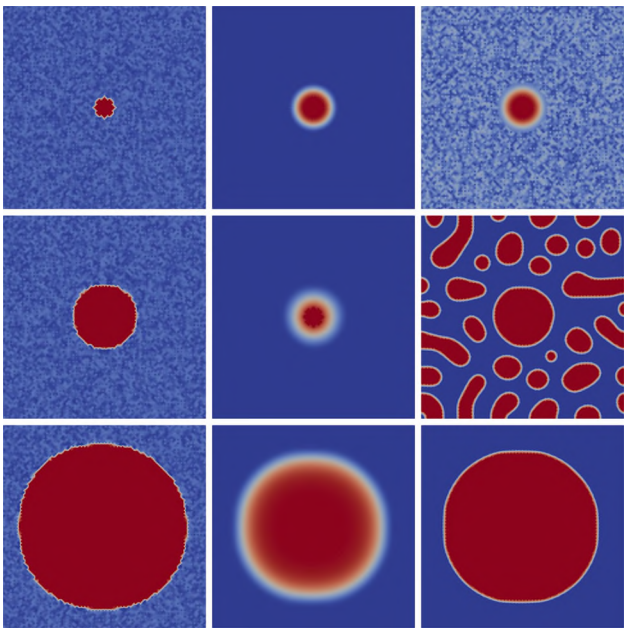

Fig. 2 Example 1: Anisotropic growth of a crystal. Orientation angle (left), local degree of crystallinity (middle), and concentration field (right) at initial time $t = 0$ s (top), at time $t = 2.07 \times 10^{-2}$ s (middle), and at time $t = 1.38 \times 10^{-1}$ s (bottom)

Figure 2 displays a top view of the three phase field variables Θ_h, ϕ_h, and c_h at initial time $t = 0$ (top), the intermediate time $t = 2.07 \times 10^{-2}$ (middle), and the time $t = 1.38 \times 10^{-1}$ (bottom). The coloring for Θ_h and ϕ_h is the same as in Fig. 1. For the concentration c_h, 'red' indicates

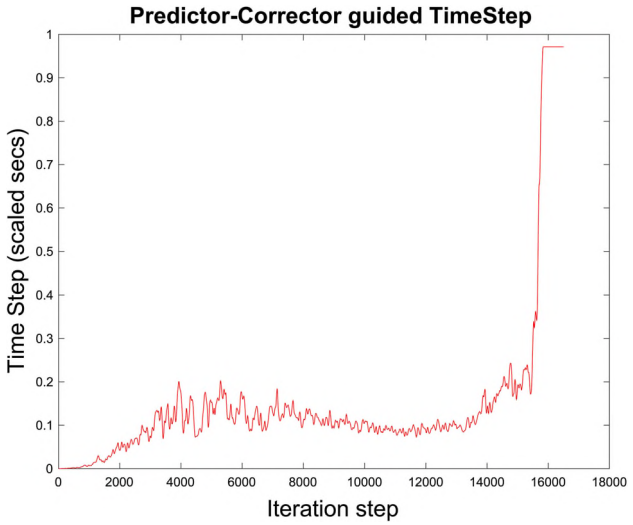

Fig. 3 Example 1: Performance of the predictor corrector continuation strategy

$c_h = 1.0$ and 'blue' stands for $c_h = 0.0$. As to be expected, the region where $c_h = 1.0$ increases according to the growth of the crystal, whereas outside that region we observe the typical spinodal decomposition for Cahn–Hilliard type equations.

The performance of the predictor corrector continuation strategy is shown in Fig. 3 which displays the adaptively chosen time step sizes as a function of the iterations. The appropriate choice of τ_m is most critical for the fully discrete Θ equation, since the original Θ equation represents a very singular diffusion process. As it turned out, the predicted time steps for the fully discrete Θ equation have been frequently rejected and subsequently reduced by the adaptive algorithm, whereas the then predicted time steps for the fully discrete ϕ and c equations have been always accepted.

Example 2 We consider the growth of four single crystals of different size and orientation which are initially occupying subdomains Ω_i, $1 \le i \le 4$, around the center of the computational domain Ω. The initial data are given by

$$\Theta_h^0 = \begin{cases} 1.2\,\pi & x \in \bar{\Omega}_1 \\ 1.0\,\pi & x \in \bar{\Omega}_2 \\ 0.8\,\pi & x \in \bar{\Omega}_3 \\ 0.6\,\pi & x \in \bar{\Omega}_4 \\ 0.9 \pm 0.05\,\pi & \text{elsewhere} \end{cases},$$

$$\phi_h^0 = \begin{cases} 1.0 & x \in \bar{\Omega}_i,\ 1 \le i \le 4, \\ 0.0 & \text{elsewhere} \end{cases},$$

$$c_h^0 = \begin{cases} 1.0 & x \in \bar{\Omega}_i \\ 0.5 \pm 0.05 & \text{elsewhere} \end{cases},$$

where the values for Θ_h^0 and c_h^0 outside $\bigcup_{i=1}^4 \bar{\Omega}_i$ are chosen randomly.

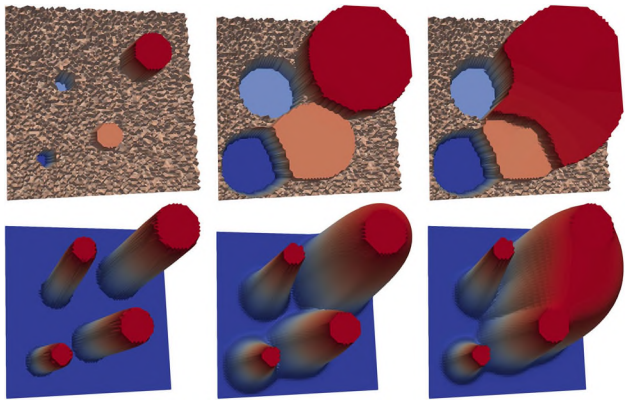

Fig. 4 Example 2: Anisotropic growth of four crystals of different size and orientation. Orientation angle (top) and local degree of crystallinity (bottom) at initial time $t = 0$ s (left), at intermediate time $t = 7.51 \times 10^{-2}$ s (middle), and at time $t = 1.54 \times 10^{-1}$ s (right)

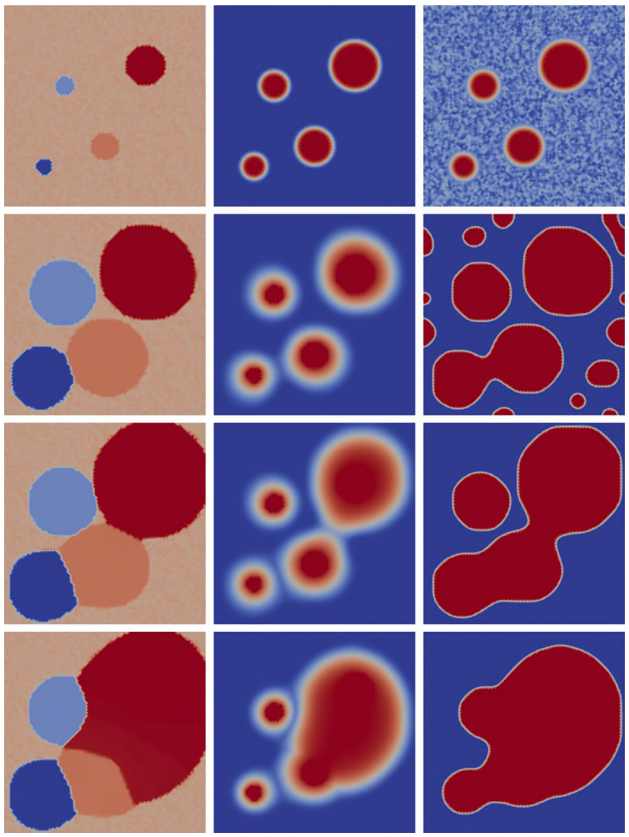

Fig. 5 Example 2: Anisotropic growth of four crystals of different size and orientation. Orientation angle (left), local degree of crystallinity (middle), and concentration field (right) at initial time $t = 0$ s (top), at intermediate times $t = 5.0 \times 10^{-2}$ s (below top), $t = 7.51 \times 10^{-2}$ s (above bottom), and at time $t = 1.54 \times 10^{-1}$ s (bottom)

Figure 4 (left) shows the initial configuration for Θ_h and ϕ_h, whereas Fig. 4 (middle) and Fig. 4 (right) display the values of these phase field variables at the intermediate time $t = 7.51 \times 10^{-2}$ s and at the time $t = 1.54 \times 10^{-1}$ s. The

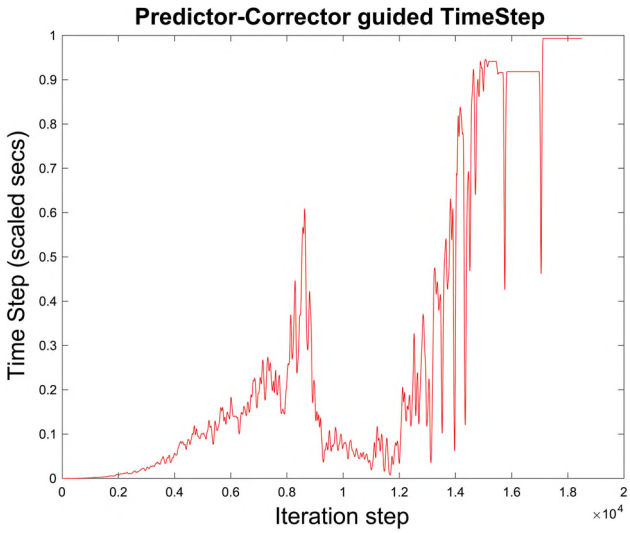

Fig. 6 Example 2: Performance of the predictor corrector continuation strategy

coloring for the local crystallinity ϕ_h is the same as in Example 1. As far as the orientation angle Θ_h is concerned, 'dark red', 'light red', 'light blue', and 'dark blue' stand for $1.2\,\pi$, $1.0\,\pi$, $0.8\,\pi$, and $0.6\,\pi$, respectively. We see the crystals grow in time [Fig. 4 (bottom middle)] with the two bigger crystals merging into each other [Fig. 4 (bottom right)]. The orientation follows the crystal growth developing upper and lower facets with narrow interfaces and steep gradients in between [Fig. 4 (top middle and top right)].

Figure 5 provides a top view of the three phase field variables Θ_h, ϕ_h, and c_h at the initial time $t = 0$ s (top), at the intermediate times $t = 5.0 \times 10^{-2}$ s (below top), $t = 7.51 \times 10^{-2}$ s (above bottom), and at the time $t = 1.54 \times 10^{-1}$ s (bottom). The coloring for Θ_h and ϕ_h is the same as in Fig. 4 and the coloring for the concentration c_h is the same as in Example 1.

Finally, Fig. 6 displays the performance of the predictor corrector continuation strategy. We observe significantly more reductions of the time step sizes as in Example 1. In particular, strong reductions occur when the domains merge into each other.

7 Conclusions

We have provided a numerical approach for the solution of a phase field model describing polycrystallization processes in binary mixtures. The three pillars of this approach are a splitting method in time, a finite element discretization in space including a C^0IPDG approximation of the Cahn–Hilliard type equation for the concentration field, and a predictor corrector continuation strategy for the numerical solution of the fully discretized problem. The numerical results illustrate that the approach is capable to capture the essential features of pattern formation in polycrystalline growth processes.

References

1. Andreu, F., Caselles, V., Mazón, J.M.: Existence and uniqueness of solutions for a parabolic quasilinear problem for linear growth functionals with L1 data. Math. Ann. **322**, 139–206 (2002)
2. Andreu-Vaillo, F., Caselles, V., Mazón, J.M.: Parabolic Quasilinear Equations Minimizing Linear Growth Functionals. Birkhäuser, Basel (2004)
3. Andreu, F., Mazòn, J.M., Segura, S., Toledo, J.: Existence and uniqueness for a degenerate parabolic equation with L1-data. Trans. Am. Math. Soc. **315**, 285–306 (1999)
4. Baldi, A.: Weighted BV functions. Houst. J. Math. **27**, 1–23 (2001)
5. Bartels, S.: Methods for Nonlinear Partial Differential Equations. Springer, Berlin (2015)
6. Bartkowiak, L., Pawlow, I.: The Cahn–Hilliard–Gurtin system coupled with elasticity. Control Cybern. **34**, 1005–1043 (2005)
7. Bebendorf, M.: A note on the Poincaré inequality for convex domains. Z. Anal. Anwend. **22**, 751–756 (2003)
8. Bellettini, G., Novaga, M., Paolini, M.: On a crystalline variational problem, part I: first variation and global L1-regularity. Arch. Ration. Mech. Anal. **157**, 165–191 (2001)
9. Bellettini, G., Novaga, M., Paolini, M.: On a crystalline variational problem, part II: BV regularity and structure of minimizers on facets. Arch. Ration. Mech. Anal. **157**, 193–217 (2001)
10. Bonetti, E., Colli, P., Dreyer, W., Giliardi, G., Schimperna, G., Sprekels, J.: On a model for phase separation in binary alloys driven by mechanical effects. Physica D **165**, 48–65 (2002)
11. Braess, D., Hoppe, R.H.W., Linsenmann, C.: A two-energies principle for the biharmonic equation and an a posteriori error estimator for an interior penalty discontinuous Galerkin approximation. ESAIM: M2AN (2016). https://doi.org/10.1051/m2an/2016074
12. Brenner, S.C., Sung, L.-Y.: C^0 interior penalty methods for fourth order elliptic boundary value problems on polygonal domains. J. Sci. Comput. **22**(23), 83–118 (2005)
13. Burger, M., Frick, K., Osher, S., Scherzer, O.: Inverse total variation flow. Multiscale Model. Simul. **6**, 365–395 (2007)
14. Carrive, M., Miranville und, A., Piétrus, A.: The Cahn–Hilliard equation for deformable elastic continua. Adv. Math. Sci. Appl. **10**, 539–569 (2000)
15. Carrive, M., Miranville, A., Piétrus, A., Rakotoson, J.: The Cahn-Hilliard equation for anisotropic deformable elastic continuum. Appl. Math. Lett. **12**, 23–28 (1999)
16. Deuflhard, P.: Newton Methods for Nonlinear Problems: Affine Invariance and Adaptive Algorithms. Springer, Berlin (2004)
17. Engel, G., Garikipati, K., Hughes, T.J.R., Larson, M.G., Mazzei, L., Taylor, R.L.: Continuous/discontinuous finite element approximations of fourth order elliptic problems in structural and continuum mechanics with applications to thin beams and plates, and strain gradient elasticity. Comput. Methods Appl. Mech. Eng. **191**, 3669–3750 (2002)
18. Feng, X., von Oehsen, M., Prohl, A.: Rate of convergence of regularization procedures and finite element approximations for the total variation flow. Numer. Math. **100**, 441–456 (2005)
19. Garcke, H.: On Cahn–Hilliard systems with elasticity. Proc. R. Soc. Edinb. Sect. A Math. **133**, 307–331 (2003)
20. Garcke, H.: On a Cahn–Hilliard system for phase separation with elastic misfit. Ann. Inst. Henri Poincaré (C) Nonlinear Anal. **22**, 165–185 (2005)

21. Giusti, E.: Minimal Surfaces and Functions of Bounded Variation. Birkhäuser, Basel (1984)
22. Gránásy, L., Börzsönyi, L., Pusztai, T.: Nucleation and bulk crystallization in binary phase field theory. Phys. Rev. Lett. **88**, 206105 (2002)
23. Gránásy, L., Börzsönyi, L., Pusztai, T.: Crystal nucleation and growth in binary phase-field theory. J. Cryst. Growth **237**, 1813–1817 (2002)
24. Gránásy, L., Pusztai, T., Börzsönyi, L., Warren, J.A., Douglas, J.F.: A general mechanism of polycrystalline growth. Nat. Mater. **3**, 645–650 (2004)
25. Gránásy, L., Pusztai, T., Warren, J.A.: Modeling polycrystalline solidification using phase field theory. J. Phys. Condens. Matter **16**, R1205–R1235 (2004)
26. Gránásy, L., Pusztai, T., Saylor, D., Warren, J.A.: Phase field theory of heterogeneous crystal nucleation. Phys. Rev. Lett. **98**, 035703 (2007)
27. Gránásy, L., Pusztai, T., Tegze, G., Warren, J.A., Douglas, J.F.: Growth and form of spherulites. Phys. Rev. E **72**, 011605 (2004)
28. Gránásy, L., Ratkai, L., Szallas, A., Korbuly, B., Toth, G., Környei, L., Pusztai, T.: Phase-field modeling of polycrystalline solidification: from needle crystals to spherulites: a review. Metall. Mater. Trans. A **45A**, 1694–1719 (2014)
29. Gurtin, M.E.: Generalised Ginzburg–Landau and Cahn–Hilliard equations based on a microforce balance. Physica D **92**, 178–192 (1996)
30. Hoppe, R.H.W., Linsenmann, C.: An adaptive Newton continuation strategy for the fully implicit finite element immersed boundary method. J. Comput. Phys. **231**, 4676–4693 (2012)
31. Kobayashi, R., Warren, J.A., Carter, W.C.: A continuum model of grain boundaries. Phys. D Nonlinear Phenom. **140**, 141–150 (2000)
32. Larché, F.C., Cahn, J.W.: The effect of self-stress on diffusion in solids. Acta Metall. **30**, 1835–1845 (1982)
33. Larché, F.C., Cahn, J.W.: The interactions of composition and stress in crystalline solids. Acta Metall. **33**, 331–357 (1985)
34. Larché, F.C., Cahn, J.W.: Phase changes in a thin plate with nonlocal self-stress effects. Acta Metall. **40**, 947–955 (1992)
35. Leo, P.H., Lowengrub, J.S., Jou, H.J.: A diffuse interface model for microstructural evolution in elastically stressed solids. Acta Mater. **46**, 2113–2130 (1998)
36. Miranville, A.: Some generalizations of Cahn–Hilliard equation. Asymptot. Anal. **22**, 235–259 (2000)
37. Miranville, A.: Long-time behavior of some models of Cahn–Hilliard equations in deformable continua. Nonlinear Anal. Real World Appl. **2**, 273–304 (2001)
38. Miranville, A.: Consistent models of Cahn–Hilliard–Gurtin equations with Neumann boundary conditions. Physica D **158**, 233–257 (2001)
39. Miranville, A.: Generalized Cahn–Hilliard equations based on a microforce balance. J. Appl. Math. **4**, 165–185 (2003)
40. Moll, S., Shirakawa, K.: Existence of solutions to the Kobayashi–Warren–Carter system. Calc. Var. Partial Differ. Equ. **51**, 621–656 (2014)
41. Moll, S., Shirakawa, K., Watanabe, H.: Energy dissipative solutions to the Kobayashi–Warren–Carter system. Nonlinearity **30**, 2752–2784 (2017)
42. Payne, L.E., Weinberger, H.F.: An optimal Poincaré inequality for convex domains. Arch. Ration. Mech. Anal. **5**, 286–292 (1960)
43. Provatas, N., Elder, K.: Phase-Field Methods in Materials Science. Wiley, Weinheim (2010)
44. Rudin, W.: Real and Complex Analysis, 3rd edn. McGraw-Hill, New York (1986)
45. Rudin, L.I., Osher, S., Fatemi, E.: Nonlinear total variation based noise removal algorithms. Phys. D Nonlinear Phenom. **60**, 259–268 (1992)
46. Tartar, L.: Introduction to Sobolev Spaces and Interpolation Theory. Springer, Berlin (2007)
47. Warren, J.A., Kobayashi, R., Carter, W.C.: Modeling grain boundaries using a phase field technique. J. Cryst. Growth **211**, 18–20 (2000)
48. Wells, G.N., Kuhl, E., Garikipati, K.: A discontinuous Galerkin method for the Cahn–Hilliard equation. J. Comput. Phys. **218**, 860–877 (2006)